Available online at www.sciencedirect.com

SciVerse ScienceDirect

Journal of the European Ceramic Society 32 (2012) 503–510

www.elsevier.com/locate/jeurceramsoc

Silicon carbide-based foams from direct blowing of polycarbosilane

Manabu Fukushima [a,b,*], Paolo Colombo [b,c]

[a] National Institute of Advanced Industrial Science and Technology (AIST), 2266-98 Shimo-Shidami, Moriyama-ku, Nagoya 463-8560, Japan
[b] Università di Padova, Dipartimento di Ingegneria Meccanica, Via Marzolo 9, 35131 Padova, Italy
[c] Department of Materials Science and Engineering, The Pennsylvania State University, University Park, PA 16802, USA

Received 20 June 2011; received in revised form 31 August 2011; accepted 12 September 2011
Available online 2 October 2011

Abstract

Macro-cellular porous silicon carbide foams were produced using a polycarbosilane preceramic polymer and a chemical blowing agent (azodicarbonamide). Polycarbosilane (PCS) was mixed with a blowing agent and the mixture was foamed close to the melting point of PCS at 250–260 °C, under nitrogen in order to avoid cross-linking by oxidation. The foamed PCS was then cured under air at 200 °C and pyrolyzed at 1000 °C, leading to the formation of open macro-cellular ceramic components. Porosity ranged from 59 to 85 vol%, and the cell size ranged from 416 to 1455 μm; these values could be modulated by changing the content of blowing agent and foaming temperature. This process is a simple and efficient way to produce silicon carbide-based foam with tailored pore architecture and porosity.

Keywords: Precursors-organic; Thermal expansion; Porosity; SiC; Macro-cellular

1. Introduction

Macrocellular ceramic components have attracted great attention due to their unique properties such as low density, low thermal conductivity, high fluid permeability, thermal shock resistance and chemical stability as well as specific strength.[1,2] These highly porous ceramics have been widely utilized in various fields such as metallurgy (molten metal filter),[3] automobile (diesel particulate filter),[4] water conservation (water purification filter and diffuser),[5,6] environmental purification or petrochemistry (catalyst support),[7] production of energy (fuel cells),[8] medical science (bioimplants)[9] as well as waste management.[10,11] The properties and performances of cellular ceramics are strongly depending on porosity, pore size, pore size distribution, pore interconnection, pore orientation and the surface of pore morphology as well as materials type. Various manufacturing processes for cellular ceramics with desired properties have been proposed, including the replica method employing polyurethane foams, the direct foaming route for ceramic suspensions or preceramic polymers, the use of sacrificial fugitives, and extrusion.[12]

It has been proposed that the use of preceramic polymers is a promising route for the fabrication of various porous structures (foams, membranes and monolithic components with hierarchical porosity).[13–29] Preceramic polymers, including organic and inorganic polymers with a continuous Si–R network (R = O, C, N and B), can provide ceramic materials as residue through their decomposition at higher temperature, where organic groups can be transformed into inorganic moieties such as Si–O, Si–C, Si–N and Si–B, usually under inert atmosphere to prevent the oxidation of organic groups. As a result, advanced ceramic materials such as SiC, Si_3N_4, SiOC, SiOCN, SiCN and SiBCN can be obtained, with microstructure and properties tailored by the molecular structure of the precursor and the pyrolysis condition.[30,31]

Among the ceramic materials prepared by preceramic polymer, SiC possesses various desired engineering properties, such as good thermal shock resistance and thermal/chemical stability as well as superior mechanical properties due to the strong covalent bonding of silicon to carbon and a low self-diffusion coefficient, indicating that it can be employed for high-temperature applications.[22,32–34] Polycarbosilane (PCS) has been extensively utilized as a representative material to obtain SiC fibers.[35,36] However, there are very few studies concerning the use of PCS to fabricate a macrocellular SiC, although there have been recent reports on the use of PCS to obtain

* Corresponding author. Tel.: +81 52 736 7426; fax: +81 52 736 7405.
E-mail address: manabu-fukushima@aist.go.jp (M. Fukushima).

0955-2219/$ – see front matter © 2011 Elsevier Ltd. All rights reserved.
doi:10.1016/j.jeurceramsoc.2011.09.009

micro-cellular[37–39] or micro-meso-porous SiC by casting[40] or nano-casting techniques.[41,42] Moreover, PCS has been used together with SiC powder to fabricate porous SiC components, obtained through simple sintering of powders[43] or by using camphene and freeze-casting.[44] Furthermore, PCS has been used to fabricate oxy-carbide porous ceramics, by emulsion processing or nano-casting.[45,46] The direct foaming technique allows a simple and economical fabrication of highly porous ceramics containing up to more than 95% porosity.[24,25,27,28,37] In the direct foaming of preceramic polymers, the SiOC, SiCN and SiOCN systems have been investigated.[24,25,27,28] Past papers suggested the reason why few studies of direct foaming PCS have been conducted, namely because the cross-linking of PCS by oxygen curing and the change in viscosity of PCS during blowing complicate the development of the macrocellular structure.[37] In particular, the relationship between the viscosity of PCS, its oxidation curing and foaming is important to prepare a porous body, and its control is still an issue to be solved for optimizing the direct foaming of PCS (and, in general, of any preceramic polymer precursor).

In this paper, we propose a very simple and promising approach to solve the above mentioned problems. Firstly, the mixture of PCS and chemical blowing agent is foamed at 250–260 °C under flowing N_2, in order to avoid the oxidation curing of PCS. We strategically selected a blowing agent based on azodicarbonamide (ADA), which can be foamed around 250 °C, which is close to the melting point of PCS (230–250 °C)[20,47,48] and produces a very high yield of gas per gram (210–230 cm^3).[49,50] This approach was firstly proposed by Takahashi and Colombo, for siloxane preceramic polymers.[51] Then, the foamed body is cured by oxidation cross linking, so that the shape of the cured body can be maintained during the subsequent pyrolysis. Finally, foamed–cured PCS bodies are pyrolyzed. The foaming process and the control over the pore architectures are here discussed, showing that by varying the processing conditions, different morphologies can be obtained.

2. Experimental

2.1. Starting materials

A commercially available PCS (Type S, Nippon Carbon Co. Ltd., Yokohama, Japan) and azodicarbonamide (ADA 97%, Sigma–Aldrich, St. Louis, MO) as a chemical blowing agent were used for the fabrication of the macrocellular SiC ceramic. The as-received powders, without further purification, were crushed into fine particles in a ball mill, in order to be homogeneously foamed.

2.2. Chemical blowing and pyrolysis

PCS/ADA solid mixtures were prepared with weight ratios of 100/0, 99/1, 97/3 and 95/5. The mixtures were put into glass beakers with an inner diameter of 17 mm, and each beaker was carefully tapped in order to level and compact the powders. Thereafter, the powder mixtures were heated up to 250 or 260 °C with a heating rate 10 °C/min and held for 2 h under N_2 flowing to induce the chemical blowing. Table 1 reports the sample identification codes, composition of the PCS/ADA mixtures and the foaming conditions. The curing of foamed PCS (oxidation cross-linking) was carried out under a heating rate of 30 °C/h to 200 °C with a hold of 2 h in static air. The foamed and cured bodies, removed from the beakers, were transferred to an alumina crucible and pyrolyzed at 1000 °C with a heating rate of 5 °C/min for 2 h in a flowing Ar atmosphere to convert the preceramic polymer to an inorganic porous SiC-based ceramic.

Table 1
Sample identification and composition of PCS/ADA mixtures, and foaming conditions.

Sample	Composition of PCS/ADA	Foaming temperature
5A0	100/0	250
5A1	99/1	
5A3	97/3	
5A5	95/5	
6A0	100/0	260
6A1	99/1	
6A3	97/3	
6A5	95/5	

2.3. Characterization

Bulk density of the tapped powder body was calculated by taking into account the mass and the dimensions of the beaker. In order to calculate the porosity of tapped body, its theoretical density was determined based on the rule of mixtures. Porosity of the foamed body at 250 or 260 °C was calculated by using the mass/dimension and true density, where true density was measured from finely ground polymer powder using a He-Pycnometer (Pycnomatic ATC, Porotec). Apparent densities, and open and closed porosity of the pyrolyzed bodies were determined by the Archimedes method using vacuum assisted water infiltration, where the true (skeleton) density of the pyrolyzed foams was measured by He picnometry (Pycnomatic ATC, Porotec) of finely ground particles. TG-DTA curves of pure ADA and PCS with ADA were obtained by a RIGAKU TG 8120 differential thermalgravimetric analyzer, at the heating rate of 10 °C/min under flowing N_2. N_2 gas was flown for 20–30 min before starting heating, in order to avoid oxygen contamination in the furnace. The porous architecture, such as cell shape, cell size and size distribution was investigated using a stereomicroscope (type 376788, Wild Heerbrugg AG, Switzerland) mounted with a digital camera (Coolpix 990, Nikon, Tokyo, Japan) and a scanning electron microscopy (SEM, JSM-6330, JEOL Techniques, Tokyo, Japan). Image analysis (PhotoMeasure, KENIS, Osaka, Japan) was used to quantify the average cell size and its distribution.

3. Results and discussion

When manufacturing macro-cellular foams using direct foaming of molten PCS, the following points need to be

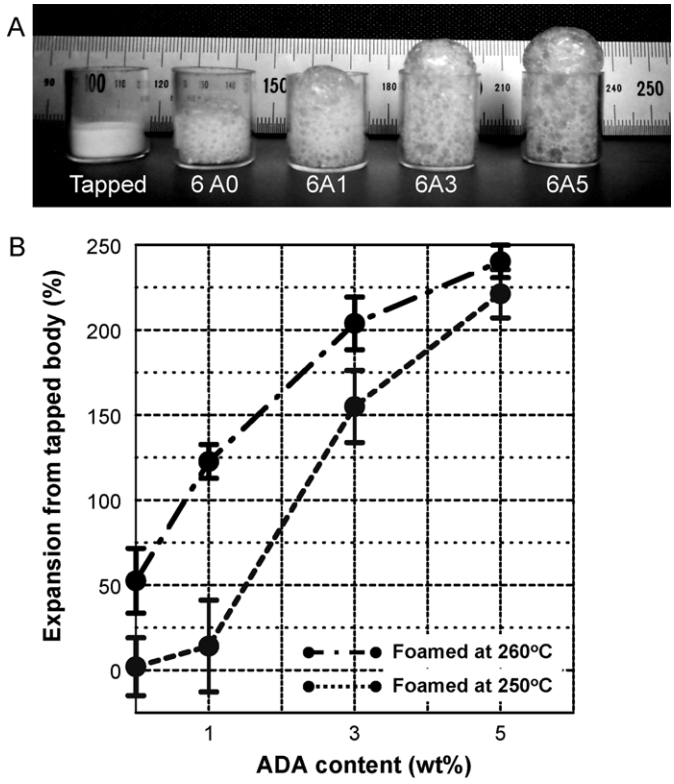

Fig. 1. (A) Photograph of foamed PCS samples, and (B) expansion as a function of ADA content and foaming temperature.

considered: (1) firstly, chemical blowing should be performed before curing, as the viscosity of the melt would increase dramatically with the formation of a rigid structure, which would require a very high pressure to sufficiently foam. Therefore, blowing under inert atmosphere is needed in order to avoid cross-linking by oxidation, (2) secondly, the fluidity of molten PCS should be adequate to retain the gas produced from the decomposition of ADA. If ADA decomposes before PCS can melt, there will be no foam formation, as the gases will escape from the polymer and (3) thirdly, after blowing, the foamed body should be cured, in order to retain the shape and morphology of the pores during the pyrolysis step. Therefore, we carried out foaming and curing on the basis of the considerations above. Because of the difficulties in cross-linking PCS, we chose to use oxidative curing, which leads to an incorporation of about 11 wt% oxygen in the final SiC ceramic.[52]

Fig. 1 reports (A) photos of PCS powder foamed at 260 °C, and (B) the expansion (%) calculated from the expanded volume to the tapped (bulk) volume ratio. The images show the homogeneous and uniform blowing of PCS, an increase in expansion (0.5 g of PCS powder was used with various ADA contents) and in the average cell size, with increasing ADA content. The volume expansion was measured according to the following equation: $100 \times (V_a - V_b)/V_b$, where V_a and V_b indicate the bulk volume of foamed PCS and the volume of tapped one (before blowing), respectively. The measured expansion was 2, 14, 155 and 221% for 5A0, 5A1, 5A3, and 5A5 samples (foamed at 250 °C), and 53, 123, 204 and 240% for the 6A0, 6A1, 6A3 and 6A5 samples (foamed at 260 °C), respectively, indicating the

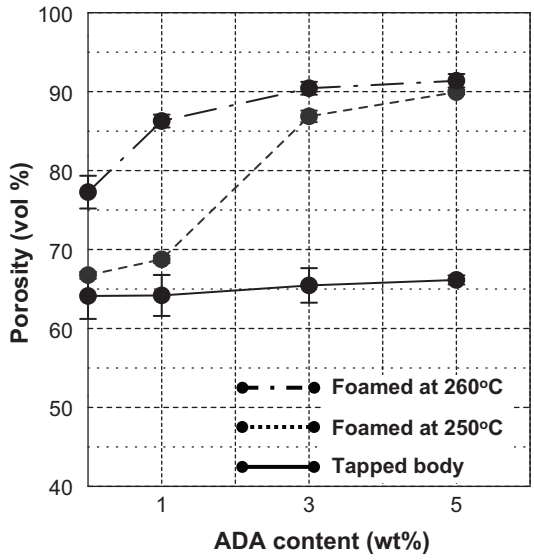

Fig. 2. Porosity of the tapped and foamed PCS bodies at 250 and 260 °C as a function of ADA amount.

increase of expansion with increasing ADA content and foaming temperature. The 5A0 and 6A0 samples (pure PCS) showed expansion after heating which was greater for the higher temperature, indicating the self-blowing of PCS due to the release of oligomeric (low molecular weight) species. Foaming was observed only when heating at fast heating rates (10 °C/min); when heating at 0.5–5 °C/min was tested in preliminary experiments, no or limited foaming was observed for the samples with or without ADA. This behavior depends on the intercorrelation between the gas evolution rate and the change in fluidity of the molten polymer, which is influenced by the decomposition rate. Therefore, the foaming schedule with a heating rate of 10 °C/min (2 h holding time) was finally selected, in order to obtain a PCS melt of suitable fluidity to retain the gas released from the decomposition of ADA. Thermal cross linking of PCS is negligible in the used blowing temperature, because PCS is thermally stable up to 350 °C.[35,52]

Fig. 2 shows the porosity of the tapped and foamed PCS bodies at 250 and 260 °C as a function of ADA amount. To measure the porosity, the bulk density (the mass to volume ratio, including the volume of open and closed porosity, and of solid skeleton) was taken into account. The porosity of the tapped body had an almost constant value, around 64–66 vol%. On the other hand, the total porosity of the foamed bodies increased remarkably with ADA content and foaming temperature, reaching 89 and 91 vol% for the 5A5 and 6A5 samples, respectively. The 5A0 and 6A0 samples (pure PCS without ADA) also showed an increase of porosity (from 64 to 67 and to 77%, respectively), suggesting once again that self-blowing occurred by the evolution of gas comprised of low molecular oligomer/volatile species and absorbed water contained in the as-received PCS. In order to investigate the decomposition of ADA and melting of PCS, TG-DTA of samples with or without ADA, to 260 °C at 10 °C/min under nitrogen flow, was carried out, and the results are shown in Fig. 3a and b. The TG curve of pure ADA showed an onset of decomposition at ~230 °C (at

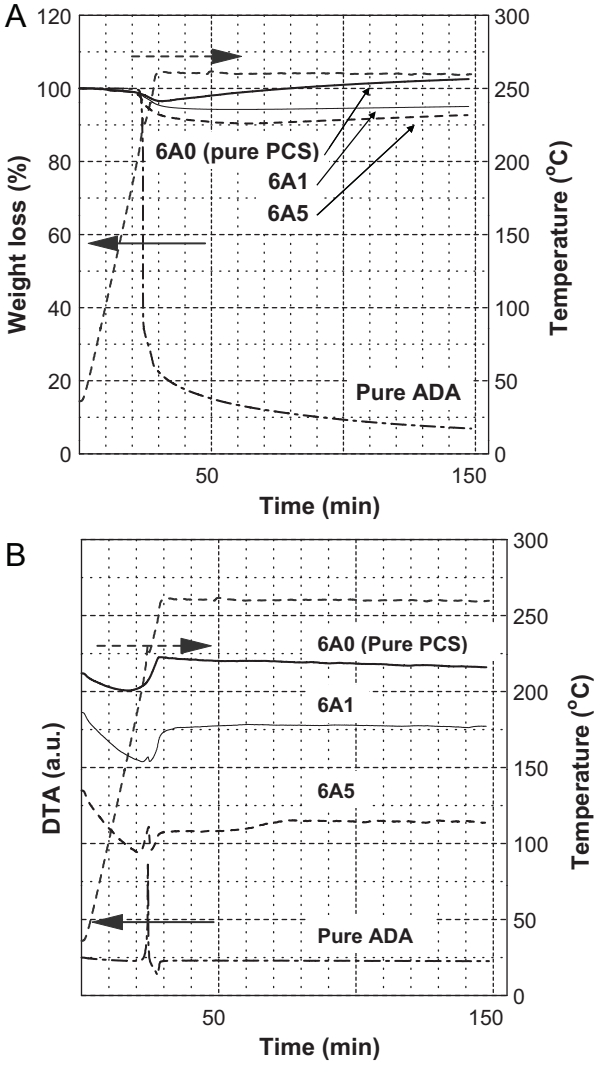

Fig. 3. (A) TG and (B) DTA curves of PCS samples with and without ADA during foaming in N_2.

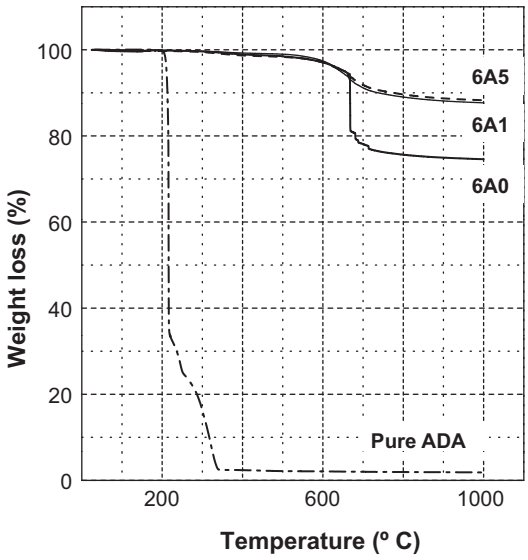

Fig. 4. TG curves of foamed PCS and pure ADA during pyrolysis.

24 min), followed by a rapid weight loss (up to 30 min, 260 °C), and further gradual loss during the holding period. Thus, the gas evolution from the decomposition of ADA occurs just after the melting of PCS. It was shown that the main gas species released in this temperature range are nitrogen (65 vol%), carbon monoxide or dioxide (32 vol%) and small amounts of NH_3, with a solid residue of 1–2 wt% comprised of urazol, biurea, cyamelide and cyanuric acid above ∼350 °C.[50] The DTA curve of pure ADA exhibited the presence of both exothermic and endothermic reactions, in accordance with what reported in the literature for this blowing agent.[53] The exothermic reaction occurred in the temperature range of 200–240 °C (21–25 min), and an endothermic peak could be observed in the temperature range of 240–260 °C (25–27 min). The exothermic and endothermic peaks observed in this study occurred at a higher temperature than that reported in the previous studies (exotherm at 170–210 °C, and endotherm at 210–230 °C), because in the present investigation we employed a higher heating rate than that of the previous studies (1–2 °C/min).[25,53] In addition to the heating rate, it was shown that the decomposition of the ADA can also depend on its particle size, the processing temperature and the presence of an activator.[25,27,49] The TG curve for pure PCS showed a weight loss onset at around 90 °C, and a weight loss of 3% at 260 °C, associated with an endothermic effect in the DTA, due to the evolution of low molecular oligomers/volatile and water.[55] At 32 min (260 °C), the start of some weight gain was observed in the TG curve, indicating the possible occurrence of some oxidative cross-linking.[55] It has already been observed, in fact, that oxygen or water could be present as impurities in the as-received PCS powder and/or the heating atmosphere, even under flowing N_2 gas.[55,56] No clear endothermic effect associated to melting could be observed, probably because this overlapped with the cross-linking. The start of weight loss for the samples containing ADA was ∼90 °C, consistent with that of pure PCS. The DTA curves showed the presence of the exothermic and endothermic effects associated to pure ADA (20–27 min). For these samples also, the TG curves showed a slight weight increase during holding at 260 °C, suggesting again the partial cross-linking by impurities in the TG furnace.

Fig. 4 shows the TG curves of foamed–cured PCS samples heated to 1000 °C under N_2 (heating rate 10 °C/min). Ceramic yields were 75, 87, and 88 wt% for 6A0, 6A1 and 6A5 samples, respectively, indicating a decrease of mass loss with increasing ADA content. This suggests the presence of some interaction between ADA and PCS, in which the azo compound presumably affects the intermolecular cross-linking reactions induced by radical species. In fact, it has been shown that the ceramic yield of polycarbosilane, polyvinylsilane and polysilazane can be improved when using azo compounds. Azo compounds lead to an increase of radical species, and therefore the cross-linking temperature decreases and the degree of cross-linking increases, through thermal cleavage of Si–H bonds.[57–60] The extraction of hydrogen and the following branching and intermolecular hydrosilylation reaction would proceed by the reaction of Si–H bond with azo-compounds, leading to the reduction of evaporable oligomers and the concurrent increase of the ceramic

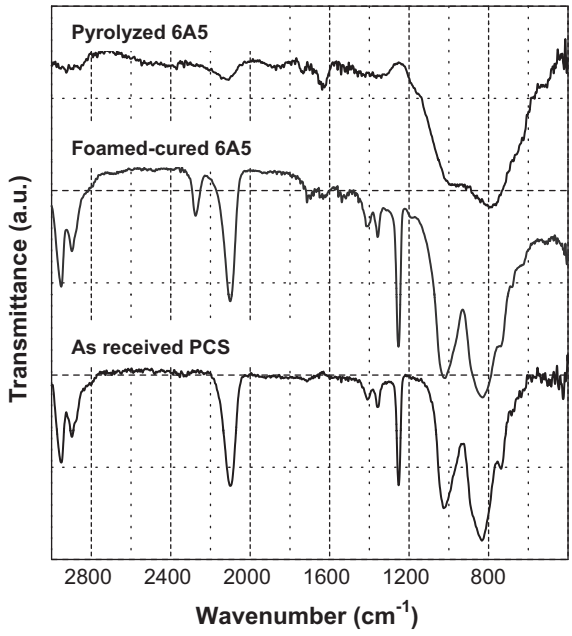

Fig. 5. FT-IR spectra of PCS before and after pyrolysis.

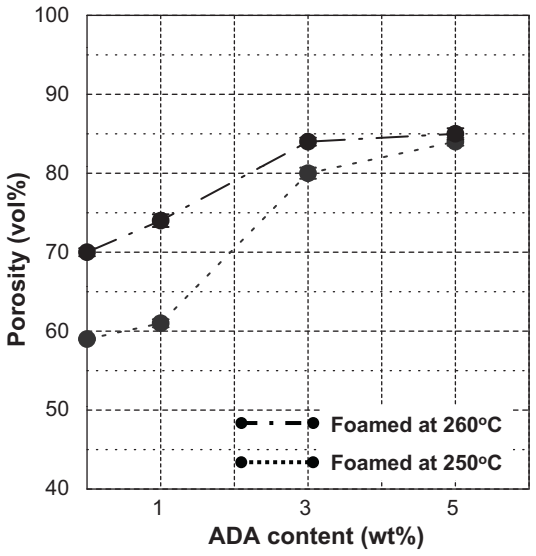

Fig. 6. Porosity of pyrolyzed foams.

yield. For instance, it has been shown that the use of 2,2-azobis(isobutyronitrile), as a radical initiator for polymerization of polyvinylsilane, led to a lowered cross-linking temperature by ~100 °C and to a higher ceramic yield.[58] More detailed investigations (comprehensive structural characterization with solid state NMR, ESR and TG–GC–MS) should be performed to clarify the mechanism of the ADA effect on the ceramic yield during pyrolysis, but this is beyond the aim of the present work. On the other hand, the TG curve of pure ADA showed a weight loss of 98.2%, indicating that the solid residue contamination produced by the decomposition of ADA within the resultant foamed ceramic was very limited.

Fig. 5 shows the FT-IR curves of as received PCS and foamed cured PCS (6A5) samples before and after pyrolysis. The typical absorption bands for pure polycarbosilane and cured PCS can be observed at 2951, 2898 (C–H stretching of Si–CH_3), 1408 (CH_2 deformation of Si–CH_3) and 1253 (Si–CH_3 deformation), 2099 (Si–H stretching), and 1357 and 1025 cm^{-1} (Si–CH_2–Si).[54] After foaming and curing, a band at 1714 (due to C=O stretching) and a small band at 1190 cm^{-1} (C–O bonds) appeared. A broad absorption band around 1100 cm^{-1} superimposed on the band around 1025 cm^{-1} was assigned to Si–O stretching in Si–O–Si or Si–O–C. These data indicate the oxidative cross linking of PCS. In addition, some peaks due to ADA were also observed, although those are less intense. There were some bands found at 2250 (overlapped with stretching cyano group from ADA residue and siloxane with Si–H bond from cured PCS) and 1720 cm^{-1} (C=O stretching from both ADA residue and cured PCS). On the other hand, during pyrolysis, the thermal decomposition of organic chains such as Si–H, Si–CH_3 and C–H occurs, accompanied by the evolution of hydrogen and hydrocarbon gases. Less intense peaks due to those organic groups were observed in the spectrum of the pyrolyzed sample, while the bands at ~1020 and 800 cm^{-1} (attributed to Si–O and Si–C stretching) can be found.[54,59] Thus, the obtained pyrolyzed foams are comprised of a SiC phase with oxygen impurities (SiO_2/SiOC phase), as expected.

Fig. 6 reports the porosity of foamed–cured–pyrolyzed PCS after pyrolysis at 1000 °C, as a function of ADA amount. Total porosity values (including open and closed porosity) increased with ADA content from 59 to 84 vol% for samples foamed at 250 °C, and from 70 to 85 vol% for samples foamed at 260 °C. Naturally, the volume of the samples after pyrolysis depends on the polymer-to-ceramic transformation, which is always accompanied by shrinkage and skeleton density increase.[59–62] The true density values for all samples were 2.25 g/cm^3, regardless of the processing route (foaming temperature and ADA content). This value is very similar to that of PCS derived SiCO fibers prepared at 1000 °C.[54,62] The apparent density, measured by He pycnometry on the pyrolyzed foam samples, was 2.14–2.15 g/cm^3, which was lower than the true density due to the presence of closed pores inside the skeleton. The amount of closed porosity was ~4–5 vol% for all pyrolyzed foams. Independent porosity measurements by the water displacement Archimedes method also showed the presence of ~4–6 vol% closed porosity. As the ADA content did not affect the amount of closed pores, their presence could be attributed mainly to meso/micro pores resulting from the pyrolysis of PCS, gas evolution and shrinkage. Isolated meso/micro pores are formed by gas evolution during pyrolysis, if the samples do not sufficiently shrink to induce pore closure. Literature data for bulk Si(O)C components prepared from PCS compact, oxidation and pyrolysis at 900 °C, indicate an amount of closed porosity of 5.7 vol%,[62] in close agreement to the values we found, indicating that the existence of closed porosity does not derive from insufficient bubble coalescence and blowing. In other words, at the chosen foaming temperature, an ADA content of 1–5 wt% is sufficient to give a macroporous cellular body based on a fully 3D interconnected open network of pores.

In order to further investigate the connectivity and macropore architecture of the samples, SEM observations were

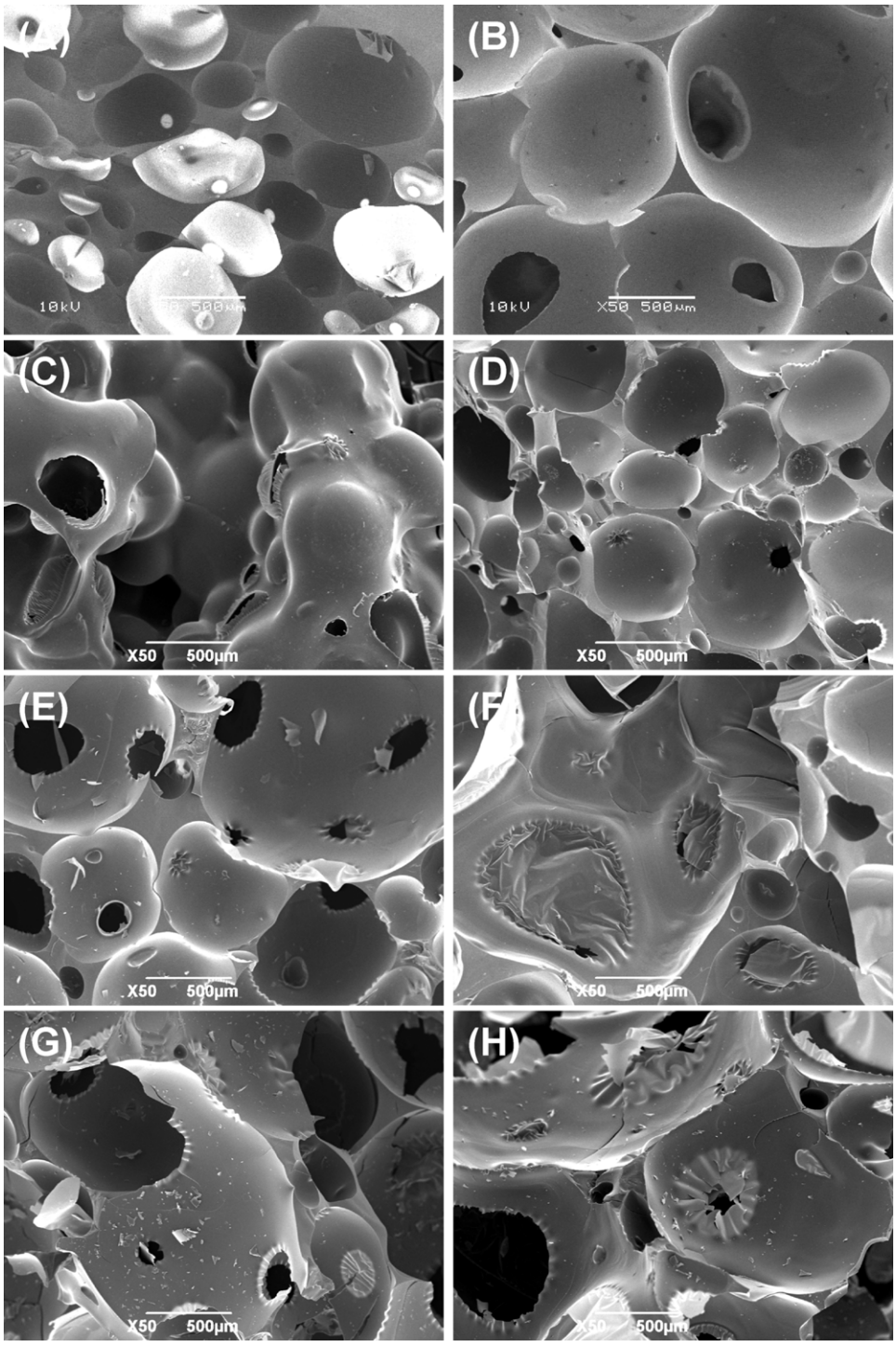

Fig. 7. Typical SEM micrographs of the fracture surface of cured 6A0 (A) and 6A5 (B) foams, and pyrolyzed 5A0 (C), 5A1 (D), 5A5 (E), 6A0 (F), 6A1 (G) and 6A5 (H) foams.

conducted, and Fig. 7 shows the typical SEM micrographs of the fracture surface of selected cured and pyrolyzed foams. After pyrolysis, partial melting was observed in the 5A0 and 6A0 samples, while the original morphology was retained in all other samples, indicating that oxygen could sufficiently diffuse into the foamed bodies during curing, and that the cross-linking achieved was enough to avoid the thermoplastic flow of PCS. No cracks were observed in the pyrolyzed foams, because this highly open porous structure enabled the steady release of the decomposition gases from PCS. The morphology is that typical for isotropic foams, comprised of homogenously distributed spherical cells, of varying size. Several cell windows were covered by thin membranes, deriving from a PCS layer left by insufficient liquid drainage at the contact point among bubbles during foaming. On the contrary, in the 5A0 sample (Fig. 7(C)), the cells were mostly closed, suggesting that the amount of gas

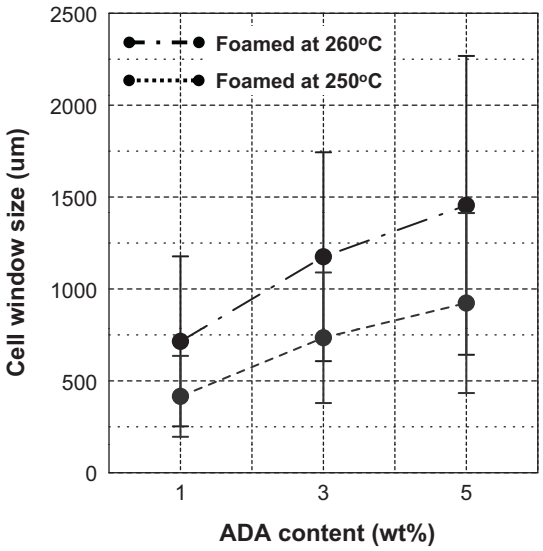

Fig. 8. Average cell size of pyrolyzed foams.

released by self foaming is insufficient to cause the formation of interconnectivity. In order to achieve that, a higher gas pressure and gas amount, such as that provided by the ADA blowing agent, are necessary. Furthermore, the insufficient degree of cross-linking observed in the 5A0 and 6A0 samples, which partially melted during pyrolysis, can be attributed to the limited permeation of oxygen through the structure during curing, due to the presence of closed cells, together with a reduced number of radical species present.

SEM investigations show that the cell wall thickness in foams produced by blowing at 260 °C is generally thinner than for samples expanded at 250 °C, because of the lower viscosity of the fluid PCS, and this results in higher total porosity values. With increasing ADA content and blowing temperature, an increase in interconnectivity among the cells could be observed. Image analysis, performed on more than 2000 cells, indicates that the 5A0 has ∼50% of open cell windows, while other all samples have over 87% of open windows, in which cells possessed at least one hole in cell wall.

The average cell size was obtained for selected samples using image analysis, according to the intercept method, and these 2D data were converted into 3D values to obtain the effective cell dimension by applying the stereological equation: $D_{sphere} = D_{circle}/0.785$.[63] The results are reported in Fig. 8. With increasing ADA content and foaming temperature, the average cell dimension tended to increase, because of higher gas pressure and lower fluid viscosity, respectively.

4. Conclusions

A novel process for the preparation of polycarbosilane derived SiC-based open cell foams, comprised of blowing under inert atmosphere to avoid cross-linking during foaming, oxidation curing and pyrolysis, has been proposed in this paper. Varying the processing conditions (amount of blowing agent and blowing temperature) resulted in cellular ceramics with total porosity in the range of 59–85 vol% and an average cell size ranging from 416 to 1455 μm. For the higher foaming temperature (260 °C), self-blowing of PCS was observed, due to the release of volatile oligomers, but the addition of a blowing agent is necessary to provide a sufficient degree of interconnectivity and an amount of porosity higher than 70 vol%.

Acknowledgements

The authors are grateful for the financial support provided by JSPS (Excellent Young Researchers Overseas Visit Program), Japan and by MIUR PRIN2008, Italy.

References

1. Colombo P, Hellmann JR, Shelleman DL. Mechanical properties of silicon oxycarbide ceramic foams. *J Am Ceram Soc* 2001;**84**(10):2245–51.
2. Colombo P, Bernardo E, Biasetto L. Novel microcellular ceramics from a silicone resin. *J Am Ceram Soc* 2004;**87**(1):152–4.
3. Taslicuku Z, Balaban C, Kuskonmaz N. Production of ceramic foam filters for molten metal filtration using expanded polystyrene. *J Eur Ceram Soc* 2007;**27**(2–3):637–40.
4. Pyzik AJ, Li CG. New design of a ceramic filter for diesel emission control applications. *Int J Appl Ceram Technol* 2005;**2**(6):440–51.
5. Wakita M. *Bull Ceram Soc Jpn* 2010;**45**:796–800 [in Japanese].
6. Zhang Y, Yu J, Chen S, Wan S. Wastewater treatment using bioreactor with dual functional ceramic membrane. *Int J Environ Pollut* 2009;**38**(3):318–27.
7. Roncari E, Galassi C, Craciun F, Capiani C, Piancastelli A. A microstructural study of porous piezoelectric ceramics obtained by different methods. *J Eur Ceram Soc* 2001;**21**(3):409–17.
8. Suzuki T, Zahir H, Funabashi Y, Yamaguchi T, Fujishiro Y, Awano M. Impact of anode microstructure on solid oxide fuel cells. *Science* 2009;**325**:852–5.
9. Le Guehennec L, Layrolle P, Daculsi G. A review of bioceramics and fibrin sealant. *Eur Cells Mater* 2004;**8**:1–11.
10. Litovsky EY, Shapiro M. Gas pressure and temperature dependences of thermal conductivity of porous ceramic materials: Part 1. Refractories and ceramics with porosity below 30%. *J Am Ceram Soc* 1992;**75**(12):3425–39.
11. Litovsky E, Shapiro M, Shavit A. Gas pressure and temperature dependences of thermal conductivity of porous ceramic materials. Part 2. Refractories and ceramics with porosity exceeding 30%. *J Am Ceram Soc* 1996;**79**(5):1366–76.
12. Colombo P. Conventional and novel processing methods for cellular ceramics. *Philos Trans R Soc A: Math Phys Eng Sci* 2006;**364**(1838):109–24.
13. Colombo P, Modesti M. Silicon oxycarbide ceramic foams from a preceramic polymer. *J Am Ceram Soc* 1999;**82**(3):573–8.
14. Schmidt H, Koch D, Grathwohl G, Colombo P. Micro-/macroporous ceramics from preceramic precursors. *J Am Ceram Soc* 2001;**84**(10):2252–5.
15. Colombo P, Bernardo E. Macro- and micro-cellular porous ceramics from preceramic polymers. *Compos Sci Technol* 2003;**63**(16):2353–9.
16. Kim Y-W, Park CB. Processing of microcellular preceramics using carbon dioxide. *Compos Sci Technol* 2003;**63**(16):2371–7.
17. Kim Y-W, Kim S-H, Kim H-D, Park CB. Processing of closed-cell silicon oxycarbide foams from a preceramic polymer. *J Mater Sci* 2004;**39**(18):5647–52.
18. Zeschky J, Höfner T, Arnold C, Weißmann R, Bahloul-Hourlier D, Scheffler M, et al. Polysilsesquioxane derived ceramic foams with gradient porosity. *Acta Mater* 2005;**53**(4):927–37.
19. Iwamoto Y, Sato K, Kato T, Inada T, Kubo Y. A hydrogen-permselective amorphous silica membrane derived from polysilazane. *J Eur Ceram Soc* 2005;**25**(2-3):257–64.
20. Nagano T, Ssto K, Saitoh T, Iwamoto Y. Gas permeation properties of amorphous SiC membranes synthesized from polycarbosilane without oxygen-curing process. *J Ceram Soc Jpn* 2006;**114**:533–8.

21. Costacurta S, Biasetto L, Pippel E, Woltersdorf J, Colombo P. Hierarchical porosity components by infiltration of a ceramic foam. *J Am Ceram Soc* 2007;**90**(7):2172–7.
22. Shibuya M, Takahashi T, Koyama K. Microcellular ceramics by using silicone preceramic polymer and PMMA polymer sacrificial microbeads. *Compos Sci Technol* 2007;**67**(1):119–24.
23. Yoon B-H, Lee E-J, Kim H-E, Koh Y-H. Highly aligned porous silicon carbide ceramics by freezing polycarbosilane/camphene solution. *J Am Ceram Soc* 2007;**90**(6):1753–9.
24. Vakifahmetoglu C, Colombo P. A direct method for the fabrication of macro-porous SiOC ceramics from preceramic polymers. *Adv Eng Mater* 2008;**10**(3):256–9.
25. Vakifahmetoglu C, Menapace I, Hirsch A, Biasetto L, Hauser R, Riedel R, et al. Highly porous macro- and micro-cellular ceramics from a polysilazane precursor. *Ceram Int* 2009;**35**(8):3281–90.
26. Vakifahmetoglu C, Colombo P, Pauletti A, Martin CF, Babonneau F. SiOC ceramic monoliths with hierarchical porosity. *Int J Appl Ceram Technol* 2010;**7**(4):528–35.
27. Vakifahmetoglu C, Pippel E, Woltersdorf J, Colombo P. Growth of one-dimensional nanostructures in porous polymer-derived ceramics by catalyst-assisted pyrolysis. Part I. Iron catalyst. *J Am Ceram Soc* 2010;**93**(4):959–68.
28. Vakifahmetoglu C, Colombo P, Carturan SM, Pippel E, Woltersdorf J. Growth of one-dimensional nanostructures in porous polymer-derived ceramics by catalyst-assisted pyrolysis. Part II. Cobalt catalyst. *J Am Ceram Soc* 2010;**93**(11):3709–19.
29. Kumar BVM, Kim Y-W. Processing of polysiloxane-derived porous ceramics: a review. *Sci Technol Adv Mater* 2010;**11**:069801.
30. Colombo P, Mera G, Riedel R, Sorarù GD. Polymer-derived ceramics: 40 years of research and innovation in advanced ceramics. *J Am Ceram Soc* 2010;**93**(7):1805–37.
31. Riedel R, Mera G, Hauser R, Klonczynski A. Silicon-based polymer derived ceramics: synthesis properties and applications: a review. *J Ceram Soc Jpn* 2006;**114**:425–44.
32. Fukushima M, Zhou Y, Yoshizawa Y, Hirao K. Water vapor corrosion behavior of porous silicon carbide membrane support. *J Eur Ceram Soc* 2008;**28**:1043–8.
33. Fukushima M, Zhou Y, Yoshizawa Y. Fabrication and microstructural characterization of porous silicon carbide with nano-sized powders. *Mater Sci Eng B* 2008;**143**:211–4.
34. Fukushima M, Zhou Y, Yoshizawa Y. Fabrication and microstructural characterization of porous SiC membrane supports with Al_2O_3–Y_2O_3. *J Membr Sci* 2009;**339**(1–2):78–84.
35. Hasegawa Y, Okamura K. Synthesis of continuous silicon carbide fibre. Part 3. Pyrolysis process of polycarbosilane and structure of the products. *J Mater Sci* 1983;**18**:3633–48.
36. Yajima S, Hayashi J, Omori M, Okamura K. Development of a silicon carbide fiber with high tensile strength. *Nature* 1976;**261**:683–5.
37. Colombo P, Hellmann JR. Ceramic foams from preceramic polymers. *Mater Res Innovat* 2002;**6**:260–72.
38. Fitzgerald TJ, Michaud VJ, Mortensen A. Processing of microcellular SiC foams. Part II. Ceramic foam production. *J Mater Sci* 1995;**30**:1037–45.
39. Kim Y-W, Kim S-H, Song I-H, Kim H-D, Park CB. Fabrication of open-cell, microcellular silicon carbide ceramics by carbothermal reduction. *J Am Ceram Soc* 2005;**88**(10):2949–51.
40. Kaskel1 S, Krawiec P. Ordered mesoporous silicon carbide. *Stud Surf Sci Catal* 2007;**170**:1770–3.
41. Sung I-K, Yoon S-B, Yu J-S, Kim D-P. Fabrication of macroporous SiC from templated preceramic polymers. *Chem Commun* 2002:1480–1.
42. Krawiec P, Geiger D, Kaskel S. Ordered mesoporous silicon carbide (OM-SiC) via polymer precursor nanocasting. *Chem Commun* 2006:2469–70.
43. Zhu S, Ding S, Xi H, Wang R. Low-temperature fabrication of porous SiC ceramics by preceramic polymer reaction bonding. *Mater Lett* 2005;**59**:595–7.
44. Yoon B-H, Park C-S, Kim H-E, Koh Y-H. In situ synthesis of porous silicon carbide (SiC) ceramics decorated with SiC nanowires. *J Am Ceram Soc* 2007;**90**:3759–66.
45. Kockrick E, Frind R, Rose M, Petasch U, Böhlmann W, Geiger D, et al. Platinum induced crosslinking of polycarbosilanes for the formation of highly porous CeO_2/silicon oxycarbide catalysts. *J Mater Chem* 2009;**19**:1543–53.
46. Krawiec P, Schrage C, Kockrick E, Kaskel S. Tubular and rodlike ordered mesoporous silicon(oxy)carbide ceramics and their structural transformations. *Chem Mater* 2008;**20**:5421–33.
47. Suwardie H, Kalyon DM, Kovenklioglu S. Thermal-behavior and curing kinetics of poly(carbosilane). *J Appl Polym Sci* 1991;**42**:1087–95.
48. Robledo-Ortiz JR, Zepeda C, Gomez C, Rodrigue D, Gonzalez-Nunez R. Non-isothermal decomposition kinetics of azodicarbonamide in high density polyethylene using a capillary rheometer. *Polym Test* 2008;**27**:730–5.
49. Quinn S. Chemical blowing agents: providing production, economic and physical improvements to a wide range of polymers. *Plast Addit Compd* 2001;**3**:16–21.
50. Lin ASP, Barrows TH, Cartmell SH, Guldberg RE. Microarchitectural and mechanical characterization of oriented porous polymer scaffolds. *Biomaterials* 2003;**24**(3):481–9.
51. Takahashi T, Colombo P. SiOC ceramic foams through melt foaming of a methylsilicone preceramic polymer. *J Por Mater* 2003;**10**:113–21.
52. Ishikawa T. Recent developments of the SiC fiber Nicalon and its composites, including properties of the SiC fiber Hi-Nicalon for ultra-high temperature. *Compos Sci Technol* 1994;**51**:135–44.
53. Lorjai P, Wongkasemjit S, Chaisuwan T. Preparation of polybenzoxazine foam and its transformation to carbon foam. *Mater Sci Eng A: Struct* 2009;**527**(1–2):77–84.
54. Hasegawa Y, Iimura M, Yajima S. Synthesis of continuous silicon carbide fibre. Part 2. Conversion of polycarbosilane fibre into silicon carbide fibres. *J Mater Sci* 1980;**15**:720–8.
55. Ly HQ, Taylor R, Day RJ, Heatley F. Conversion of polycarbosilane(PCS) to SiC-based ceramic. Part 1. Characterisation of PCS and curing products. *J Mater Sci* 2001;**36**:4037–43.
56. Suwardie H, Kalyon KM, Kovenklioglu S. Thermal behavior and curing kinetics of poly(carbosilane). *J Appl Polym Sci* 1991;**42**:1087.
57. Yu Z, Zhan J, Huang M, Li R, Zhou C, He G, et al. Preparation of a hyperbranched polycarbosilane precursor to SiC ceramics following an efficient room-temperature cross-linking process. *J Mater Sci* 2010;**45**:6151–8.
58. Itoh M, Iwata K, Kobayashi M, Takeuchi R, Kabeya T. Preparations and properties of poly(vinylsilane)s. *Macromolecules* 1998;**31**:5609–15.
59. Bouillon E, Langlais F, Pailler R, Naslain R, Cruege F, Huong PV, et al. Conversion mechanisms of a polycarbosilane precursor into an SiC-based ceramic material. *J Mater Sci* 1991;**26**(5):1333–45.
60. Ly HQ, Taylor R, Day RJ, Heatley F. Conversion of polycarbosilane(PCS) to SiC-based ceramic. Part II. Pyrolysis and characterization. *J Mater Sci* 2001;**36**:4045–457.
61. Yajima S, Hayashi J, Omori M. Continuous silicon carbide fiber of high tensile strength. *Chem Lett* 1975:931–4.
62. Li Y-Li, Fan H, Su D, Fasel C, Riedel R. Synthesis, structures, and properties of bulk Si(O)C ceramics from polycarbosilane. *J Am Ceram Soc* 2009;**92**(10):2175–81.
63. ASTM D 3576. Standard test method for cell size of rigid cellular plastics. Annual Book of ASTM Standards, vol. 08.02. West Conshohocken, PA, 1997.